

Neutron-diffraction study of $\text{Tl}_2\text{Ba}_2\text{CuO}_{6+\delta}$ with various T_c 's from 0 to 73 K

Y. Shimakawa, Y. Kubo, T. Manako, and H. Igarashi

Fundamental Research Laboratories, NEC Corporation, 4-1-1 Miyazaki, Miyamae-ku, Kawasaki 213, Japan

F. Izumi

National Institute for Research in Inorganic Materials, 1-1 Namiki, Tsukuba 305, Japan

H. Asano

Institute of Materials Science, University of Tsukuba, Tennodai, Tsukuba 305, Japan

(Received 14 June 1990)

We refined the crystal structures of four pseudotetragonal samples of $\text{Tl}_2\text{Ba}_2\text{CuO}_{6+\delta}$ with T_c 's of 0 (metallic), 48, 58, and 73 K by Rietveld analysis of time-of-flight neutron-powder-diffraction data. The presence of excess oxygen atoms located at an interstitial site between double TlO layers was confirmed. The change in oxygen content and the corresponding one in hole carrier concentration in this compound are caused by incorporation and release of the excess oxygen, whose amount is about 0.1 per formula unit for the metallic nonsuperconducting sample. The highest T_c value of about 85 K in $\text{Tl}_2\text{Ba}_2\text{CuO}_{6+\delta}$ is achieved in the absence of excess oxygen. As the oxygen content is decreased, the c value increases, and apical O^{2-} ions go away from the CuO_2 layer, while Ba^{2+} ions approach it. It was also suggested that about 5% of a Tl site is substituted by Cu. A significant portion of hole carriers in this compound is attributed to substitution of Cu for Tl and incorporation of excess oxygen.

INTRODUCTION

A Tl-containing oxide with the ideal composition of $\text{Tl}_2\text{Ba}_2\text{CuO}_6$ (Tl 2:2:0:1) is one of the most tempting materials in oxide superconductors because it shows wide T_c variation from 0 to over 85 K without significant changes in the crystal structure. We first pointed out that this T_c variation is caused by a small change in oxygen content.¹ A fully oxygenated sample is a metallic nonsuperconductor, while Ar reduction gives rise to superconductivity. Since the change in oxygen content causes the change in carrier concentration, these facts mean that the increase in carrier concentration lowers T_c in this oxide, which was confirmed by both Hall-coefficient and resistivity measurements.² Thus, Tl 2:2:0:1 is overdoped with hole carriers, and excess hole carriers suppress superconductivity.

The phenomenon that superconductivity is degraded if the carrier concentration exceeds an optimum value was first reported for $(\text{La}_{1-x}\text{Sr}_x)_2\text{CuO}_4$.³ Similar behavior was also observed in $\text{Tl}(\text{La}_{1-x}\text{Ba}_x)_2\text{CuO}_5$.⁴ These findings have established the idea that superconductivity appears only in a certain appropriate range of carrier concentration lying between an antiferromagnetic insulator and a normal metal. Most studies have dealt with the insulator-superconductor transitions, whereas studies on the metal-superconductor transition have been restricted to $(\text{La}_{1-x}\text{Sr}_x)_2\text{CuO}_4$ so far.^{5,6} Tl 2:2:0:1 provides a novel example of the metal-superconductor transition. Moreover, it shows much higher transition temperatures, up to 85 K, than the La-Sr-Cu-O and Tl-La-Ba-Cu-O systems.

Previous work^{2,7} revealed that a decrease in oxygen

content of about 0.1 per formula unit of $\text{Tl}_2\text{Ba}_2\text{CuO}_6$, which corresponds to a decrease in hole concentration of 0.2, raises T_c up to about 80 K and increases the c value by about 0.4%. It was also found that spacings between metal sheets are correlated with changes in T_c .¹ Then, the following questions are raised. Where is oxygen incorporated and released? How do metal-oxygen interatomic distances vary with the oxygen content? Are there any excess oxygen atoms in this compound? These questions should be answered to understand the superconducting mechanism of Tl 2:2:0:1. In the present study, the crystal structures of Tl 2:2:0:1 with four different T_c 's were refined by Rietveld analysis of neutron-powder-diffraction data with the auxiliary use of x-ray-powder-diffraction data. We have now clarified systematic structural changes accompanying changes in oxygen content. We will also discuss the origin of hole doping in this compound.

EXPERIMENT

Tl 2:2:0:1 samples with apparent tetragonal symmetry were prepared by solid-state reactions similar to those described in Refs. 1 and 7. In preliminary experiments, several samples with compositions around the stoichiometric one ([Tl]:[Ba]:[Cu]=2:2:1) were synthesized to obtain a pure sample. Judging from neutron- and x-ray-diffraction measurements, a single-phase tetragonal sample was obtained only for a starting composition close to [Tl]:[Ba]:[Cu]=2:2:1.1, while very small peaks of $\text{Tl}_2\text{Ba}_2\text{O}_5$ were detected in the stoichiometric sample. Thus samples with the starting compositional ra-

tio of [Tl]:[Ba]:[Cu]=2:2:1.1 were used in this study. Their oxygen contents were controlled by changing annealing conditions in a similar manner to that described in Ref. 7.

Neutron-diffraction data were taken on a high-resolution time-of-flight (TOF) neutron powder diffractometer, HRP,⁸ at the KENS pulsed spallation neutron source at the National Laboratory for High Energy Physics. The sample was contained in a cylindrical V cell 5 mm in radius, 42 mm in height, and 25 μm in thickness and placed in an Al vacuum chamber. The cell was kept rotating around its axis during data collection. Intensity data were measured at room temperature using twelve ³He counters installed with an average 2θ of 170° and then time focused by off-line data processing. The dependence of the incident intensity on TOF, t , was monitored during data collection with a fission chamber. This spectrum $C_m(t)$ was smoothed by the combination of Fourier transform, low-pass filtering, and inverse Fourier transform. X-ray diffraction data were collected using Cu $K\alpha$ radiation with a curved graphite monochromator. The step width was 0.02° in 2θ , and the scanning range was 20° – 100° . The neutron- and x-ray-diffraction data were analyzed using a Rietveld refinement program RIETAN.^{9,10}

RESULTS AND DISCUSSION

As shown in Fig. 1, four samples used for the neutron- and x-ray-diffraction measurements had different T_c 's of 0, 48, 58, and 73 K. All the samples gave diffraction patterns containing only Tl 2:2:0:1 peaks in both the neutron- and x-ray-diffraction measurements.

As described above, the Cu-rich starting composition is necessary to obtain a pure sample. X-ray microanalysis indicated that the Tl 2:2:0:1 phase has, independent of the starting composition, slightly Tl-poor and Cu-rich compositions, typically [Tl]:[Ba]:[Cu]=1.85–1.90:2:1.15–1.10, suggesting a possible substitution of Cu for Tl. Since the coherent scattering length of Tl (8.776 fm) is rather similar to that of Cu (7.718 fm), it is difficult to confirm such a substitution by neutron diffraction. Thus, the neutron-diffraction data were analyzed by fixing the composition at

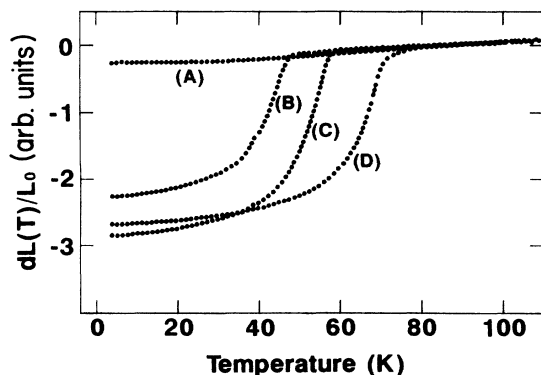


FIG. 1. Temperature dependence of the ac susceptibility for the four Tl 2:2:0:1 samples.

($\text{Tl}_{0.95}\text{Cu}_{0.05}$)₂Ba₂CuO₇, which was consistent with the starting composition except for the content of the evaporable element Tl. We wish to point out that the values of refined parameters do not depend so much on the [Cu]:[Tl] ratio because of the small difference in scattering length between Cu and Tl. We will discuss the details of the substitution for Cu and Tl in relation to hole carrier concentrations in this compound later.

The crystal structures of the four samples were analyzed based on the tetragonal space group of $I4/mmm$. An initial structural model was based on that proposed by Torardi *et al.*,¹¹ and site names in this paper follow their nomenclature. Preliminary refinements assigned isotropic thermal parameters B for all the sites. A resulting large isotropic thermal parameter for O(3), which was first located at an ideal $4e$ position, was suggestive of static displacements of this oxygen atom. Thus the O(3) atom was split into four pieces by assigning a $16n$ site deviating slightly from the ideal site. Moreover, as shown in Fig. 2, the partial occupation of an interstitial O(4) site between double TlO layers, similar to those observed in La₂CuO_{4+ δ} (Ref. 12) and La₂NiO_{4+ δ} (Ref. 13), was detected by neutron diffraction. Occupation of a similar interstitial oxygen site was also proposed in orthorhombic Tl 2:2:0:1 by Parise *et al.*¹⁴ The O(4) atom was then assigned at an $8g$ site ($0, \frac{1}{2}, z$) close to a $4d$ site ($0, \frac{1}{2}, \frac{1}{4}$), and its isotropic thermal parameter was fixed at 1.0 in the same way as in the case of La₂NiO_{4+ δ} .¹³ Finally, anisotropic thermal parameters were given to sites Tl, Ba, Cu, O(1), O(2), and O(3).

The results of the refinements for the four samples are listed in Tables I–IV. Typical Rietveld refinement patterns are shown in Fig. 3. Important crystal data including lattice parameters, site occupancies, and interatomic distances are listed in Table V.

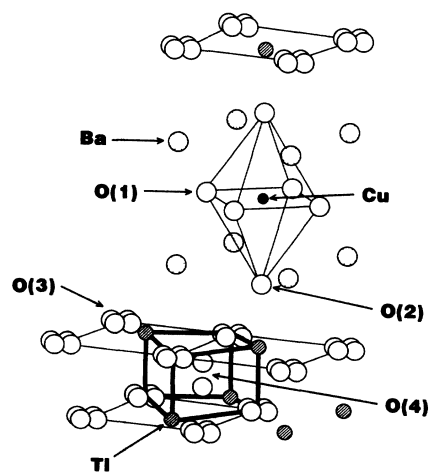


FIG. 2. Crystal structure of Tl 2:2:0:1. The O(3) atom is split into four pieces by assigning a $16n$ site deviating slightly from the ideal site. The O(4) atom is located at the interstitial site between double TlO layers. Each O(4) atom is coordinated to four Tl atoms, and is split into two pieces by assigning an $8g$ site.

TABLE I. Crystallographic data for $\text{Ti}_2\text{Ba}_2\text{CuO}_{6+\delta}$. All the atoms except for O(4) were assigned anisotropic thermal parameters. g is the occupation factor. U_{ij} 's are anisotropic thermal parameters when the temperature factor is defined as $\exp\{-2\pi^2[h^2a^2U_{11} + k^2b^2U_{22} + l^2c^2U_{33} + 2(hka^2*U_{12} + klb^2*U_{13} + klc^2*U_{23})]\}$, B_{eq} is the equivalent isotropic thermal parameter. Numbers in parentheses are uncertainties in the last decimal place. The isotropic thermal parameter of the O(4) site was fixed at 1.0. Sample A ($T_c = 0$ K): $a = 3.86298(7)$ Å, and $c = 23.1369(5)$ Å. Note that $R_{\text{up}} = 4.23\%$, $R_p = 3.28\%$, $R_f = 3.93\%$, $R_e = 3.08\%$, and $R_g = 3.72\%$. Composition determined by these data is $(\text{Ti}_{0.95}\text{Cu}_{0.05})_2\text{Ba}_2\text{CuO}_{6.080}$.

Atom	Site	x	y	z	g	U_{11} (Å ²)	U_{22} (Å ²)	U_{33} (Å ²)	U_{13} (Å ²)	B_{eq} (Å ²)
$\text{Ti}_{0.95}\text{Cu}_{0.05}$	4e	0.0	0.0	0.29740(8)	1.0	0.0261(6)	0.0261	0.0074(8)	0.0	1.57
Ba	4e	0.0	0.0	0.0842(1)	1.0	0.0064(7)	0.0064	0.0142(14)	0.0	0.71
Cu	2b	0.0	0.0	0.5	1.0	0.0049(7)	0.0049	0.0131(14)	0.0	0.60
O(1)	4c	0.0	0.5	0.0	1.0	0.0070(11)	0.0082(11)	0.0130(13)	0.0	0.74
O(2)	4e	0.0	0.0	0.3832(1)	1.0	0.0179(8)	0.0179	0.0096(13)	0.0	1.20
O(3)	16n	0.0	0.096(4)	0.2098(2)	0.246(3)	0.047(8)	0.083(12)	0.008(2)	0.011(8)	3.61
O(4)	8g	0.0	0.5	0.267(2)	0.028(3)					1.0

TABLE II. Same as for Table I, but for sample B ($T_c = 48$ K): $a = 3.86276(6)$ Å, and $c = 23.1848(4)$ Å. Note that $R_{\text{up}} = 3.97\%$, $R_p = 3.08\%$, $R_f = 3.16\%$, $R_e = 2.58\%$, and $R_g = 3.41\%$. Composition determined by these data is $(\text{Ti}_{0.95}\text{Cu}_{0.05})_2\text{Ba}_2\text{CuO}_{6.080}$.

Atom	Site	x	y	z	g	U_{11} (Å ²)	U_{22} (Å ²)	U_{33} (Å ²)	U_{13} (Å ²)	B_{eq} (Å ²)
$\text{Ti}_{0.95}\text{Cu}_{0.05}$	4e	0.0	0.0	0.29739(8)	1.0	0.0233(6)	0.0233	0.0065(8)	0.0	1.40
Ba	4e	0.0	0.0	0.0834(1)	1.0	0.0065(7)	0.0065	0.0117(13)	0.0	0.65
Cu	2b	0.0	0.0	0.5	1.0	0.0040(7)	0.0040	0.0118(13)	0.0	0.52
O(1)	4c	0.0	0.5	0.0	1.0	0.0063(11)	0.0084(11)	0.0114(12)	0.0	0.69
O(2)	4e	0.0	0.0	0.3830(1)	1.0	0.0168(8)	0.0168	0.0079(13)	0.0	1.09
O(3)	16n	0.0	0.090(3)	0.2105(2)	0.250(3)	0.030(6)	0.057(8)	0.010(2)	0.016(6)	2.53
O(4)	8g	0.0	0.5	0.270(3)	0.020(3)					1.0

TABLE III. Same as for Table I, but for sample C ($T_c = 58$ K): $a = 3.86273(6)$ Å, and $c = 23.1995(4)$ Å. Note that $R_{wp} = 4.21\%$, $R_p = 3.25\%$, $R_f = 3.30\%$, $R_I = 2.54\%$, and $R_e = 3.17\%$. Composition determined by these data is $(\text{Ti}_{0.95}\text{Cu}_{0.05})_2\text{Ba}_2\text{CuO}_{6.044}$.

Atom	Site	x	y	z	g	U_{11} (Å ²)	U_{22} (Å ²)	U_{33} (Å ²)	U_{13} (Å ²)	B_{eq} (Å ²)
Ti _{0.95} Cu _{0.05}	4e	0.0	0.0	0.2975(1)	1.0	0.0233(7)	0.0233	0.0058(9)	0.0	1.38
Ba	4e	0.0	0.0	0.0833(1)	1.0	0.0075(9)	0.0075	0.0109(15)	0.0	0.68
Cu	2b	0.0	0.0	0.5	1.0	0.0029(9)	0.0029	0.0116(16)	0.0	0.46
O(1)	4c	0.0	0.5	0.0	1.0	0.0074(13)	0.0074(13)	0.0102(15)	0.0	0.66
O(2)	4e	0.0	0.0	0.3829(1)	1.0	0.0174(10)	0.0174	0.0066(15)	0.0	1.09
O(3)	16n	0.0	0.091(3)	0.2106(2)	0.247(4)	0.019(5)	0.047(8)	0.010(3)	-0.0007(71)	2.00
O(4)	8g	0.0	0.5	0.269(4)	0.017(4)					1.0

TABLE IV. Same as for Table I, but for sample D ($T_c = 73$ K): $a = 3.86248(6)$ Å, and $c = 23.2248(4)$ Å. Note that $R_{wp} = 4.10\%$, $R_p = 3.19\%$, $R_f = 3.17\%$, $R_I = 2.74\%$, and $R_e = 3.85\%$. Composition determined by these data is $(\text{Ti}_{0.95}\text{Cu}_{0.05})_2\text{Ba}_2\text{CuO}_{5.996}$.

Atom	Site	x	y	z	g	U_{11} (Å ²)	U_{22} (Å ²)	U_{33} (Å ²)	U_{13} (Å ²)	B_{eq} (Å ²)
Ti _{0.95} Cu _{0.05}	4e	0.0	0.0	0.29744(6)	1.0	0.0212(4)	0.0212	0.0069(6)	0.0	1.30
Ba	4e	0.0	0.0	0.08299(8)	1.0	0.0067(5)	0.0067	0.0101(9)	0.0	0.62
Cu	2b	0.0	0.0	0.5	1.0	0.0024(5)	0.0024	0.0113(10)	0.0	0.43
O(1)	4c	0.0	0.5	0.0	1.0	0.0047(6)	0.0082(8)	0.0104(9)	0.0	0.61
O(2)	4e	0.0	0.0	0.38285(8)	1.0	0.0157(6)	0.0157	0.0061(9)	0.0	0.98
O(3)	16n	0.0	0.081(2)	0.2109(1)	0.247(2)	0.020(3)	0.035(4)	0.011(1)	0.007(5)	1.72
O(4)	8g	0.0	0.5	0.267	0.005(2)					1.0

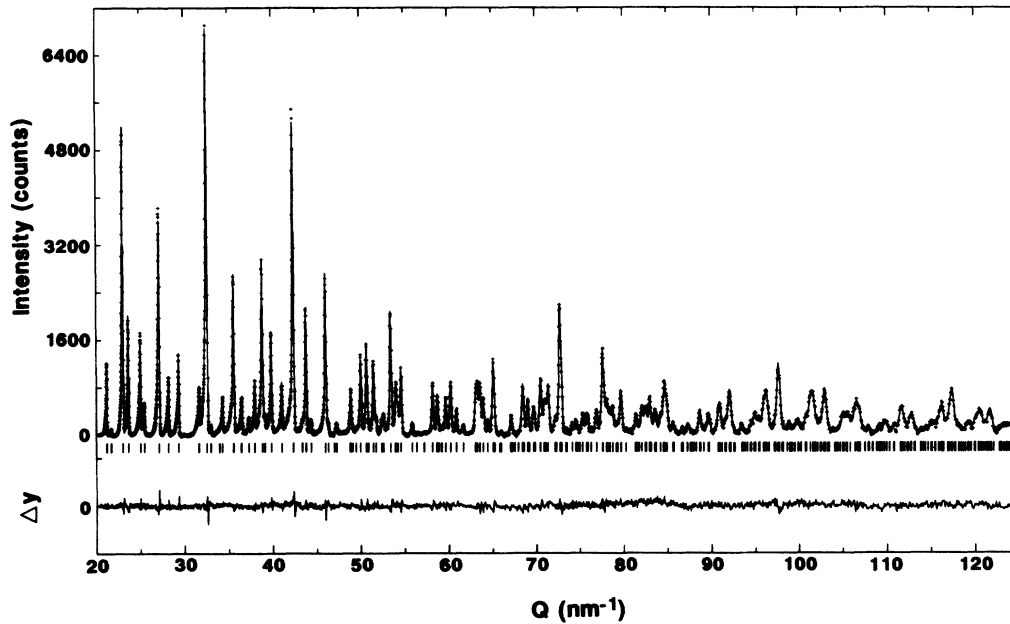


FIG. 3. Rietveld refinement patterns for Tl 2:2:0:1 with T_c of 48 K (sample *B*) plotted against $Q (= 2\pi/d)$. The background is subtracted. Plus marks are observed neutron-diffraction intensities, and solid lines are calculated intensities. Vertical marks below the profile indicate the positions of the 484 allowed reflections. The curve at the bottom is the difference between the observed and calculated intensities in the same scale.

A systematic change in the occupancy of the O(4) site is worth noting. As the T_c value increases, the occupancy of the O(4) site decreases monotonously. In contrast, the occupancies of the O(3) site are very close to 0.25 irrespective of their T_c values. Thus, the O(3) site on the rock-salt type TlO layer is almost fully occupied, and the oxygen content in Tl 2:2:0:1 is controlled by the reversible incorporation of the interstitial O(4) site. The reversible incorporation of the oxygen atoms between the double TlO layers in this oxide is supported by the previous observation that the TlO-monolayer compound, TlLaBa-

gen content.⁷ The presence of the interstitial oxygen atoms are also suggested by the local displacement of the O(3) atom. The degree of displacement for the O(3) atom from the ideal site increases as the occupancy of the O(4) site increases. Thus, the interstitial oxygen atoms repel neighboring O(3) atoms to increase distances between two O(3) atoms. On the other hand, two O(3) atoms come closer to each other if a neighboring O(4) site is vacant.

The difference in oxygen content between the samples with T_c 's of 0 K (*A*) and 73 K (*D*) is -0.084 per formula

TABLE V. Lattice parameters (Å), occupation factors, oxygen content, and metal-oxygen interatomic distances (Å) in the four samples of Tl 2:2:0:1.

	Samples				$\frac{D-A}{A} \times 100$
	<i>A</i> (0 K)	<i>B</i> (48 K)	<i>C</i> (58 K)	<i>D</i> (73 K)	
<i>a</i>	3.862 98(7)	3.862 76(6)	3.862 73(6)	3.862 48(6)	-0.013
<i>c</i>	23.136 9(5)	23.184 8(4)	23.199 5(4)	23.224 8(4)	0.380
<i>g</i> (O(3))	0.246(3)	0.250(3)	0.247(4)	0.247(2)	
<i>g</i> (O(4))	0.028(3)	0.020(3)	0.017(4)	0.005(2)	
6+ δ	6.080	6.080	6.044	5.996	(-0.084) ^a
Cu-O(1) ($\times 4$)	1.931 49(4)	1.931 38(3)	1.931 37(3)	1.931 24(3)	-0.025
Cu-O(2) ($\times 2$)	2.703(3)	2.713(3)	2.716(3)	2.721(2)	0.666
Ba-O(1) ($\times 4$)	2.743(2)	2.733(2)	2.733(2)	2.729(1)	-0.510
Ba-O(2) ($\times 4$)	2.834 1(8)	2.840 4(8)	2.841 1(10)	2.844 1(6)	0.353
Ba-O(3) ($\times \frac{1}{4} \times 4$) ^b	2.929(5)	2.968(5)	2.972(6)	2.987(3)	1.980
Tl-O(2)	1.985(3)	1.985(3)	1.983(4)	1.984(2)	-0.050
Tl-O(3) ($\times \frac{1}{4} \times 8$) ^b	2.490(10)	2.504(7)	2.501(6)	2.526(4)	1.446
Tl-O(3) ($\times \frac{1}{4} \times 8$) ^b	3.009(11)	2.994(8)	2.997(7)	2.968(5)	-1.363
Tl-O(3) ($\times \frac{1}{4} \times 4$) ^b	2.061(5)	2.044(5)	2.047(5)	2.034(3)	-1.310

^aThe difference in oxygen content between samples *A* and *D*.

^bThe O(3) atom is split into four pieces.

unit. This value agrees well with an experimental value of about -0.08 obtained by a weight-change measurement.⁷ Since sample *D* ($T_c = 73$ K) scarcely has excess oxygen at the O(4) site, the highest T_c value of about 85 K must be achieved in the sample with no interstitial oxygen atoms. This also agrees with the previous result that the sample with the highest T_c tends to decompose by further reduction.⁷ Consequently, the formula of this compound should be expressed as $(\text{Tl}_{0.95}\text{Cu}_{0.05})_2\text{Ba}_2\text{CuO}_{6+\delta}$ ($\delta \sim 0-0.1$).

We cannot find any structural discontinuity in the change from a normal-metal (nonsuperconductor) to a superconductor. As the T_c value increases, i.e., the oxygen content decreases, the a value decreases only slightly, whereas the c value increases considerably by 0.38% between samples *A* and *D*. Corresponding changes in interatomic distances along the [001] direction are specially noted. The distance between Cu and apical O(2) increases by 0.67%, which is twice the increase of that in c . In contrast, the Ba atom approaches the CuO_2 layer by as much as 1.06%, which makes the BaO layer much rougher. These structural changes are quite reasonable because the release of oxygen atoms decreases the hole carriers (positive charge) in the CuO_2 layer. Consequently, negatively charged apical O^{2-} ions are repulsed and go away from the CuO_2 layer, while positively charged Ba^{2+} ions are attracted and approach it.

Local displacement of the O(3) atom from the ideal position must be indispensable for the relaxation of a dimensional mismatch between the TlO and CuO_2 layers. Since the overall cell dimension is mainly controlled by the stiffer CuO_2 layer, the TlO layer must be "stretched." Then, the oxygen atoms on the TlO layer must relax from their ideal positions to achieve more desirable bond lengths. Such static displacements of the O(3) atoms make interstitial spaces large enough to accommodate the excess O(4) atoms. Possible displacements of the Tl atom are also suggested by its large and anisotropic thermal vibrations ($U_{11} = U_{22} > U_{33}$), which seems to reflect the deviation of this atom from the ideal site. In an orthorhombic sample, such local displacements of the O(3) and Tl atoms evidently occur along a [010] direction and cause macroscopically orthorhombic symmetry.¹⁴ Since the pseudotetragonal samples consist of short-range-ordered orthorhombic microdomains as observed by transmission electron microscopy,¹ the apparent anisotropic thermal vibrations seem to reflect the marked displacements along the [010] direction in the orthorhombic microdomains. Orthorhombic distortion and weak modulation must be, for the most part, associated with such local displacements of O(3) and Tl atoms.

Finally, we will discuss the origin of hole doping in this compound. The Tl 2:2:0:1 compound should contain no carrier if it has the stoichiometric composition of $\text{Tl}_2\text{Ba}_2\text{CuO}_6$. However, substitution of Cu^+ and/or Cu^{2+} ions for Tl^{3+} ions plus incorporation of O(4) atoms must produce hole carriers. The substitution of Cu for Tl was confirmed by Rietveld analysis of x-ray-diffraction data. The value of x in the $\text{Tl}_{1-x}\text{Cu}_x$ site was refined to be 0.033, which is close to the composition of $(\text{Tl}_{0.95}\text{Cu}_{0.05})_2\text{Ba}_2\text{CuO}_{6+\delta}$ used in the neutron Rietveld

refinements. Single-crystal x-ray analysis has also suggested substitution of Cu for Tl in $\text{Tl}_2\text{Ba}_2\text{CaCu}_2\text{O}_8$.¹⁵ In addition, even the single-phase samples used in this study showed large Curie-like susceptibility. A possible interpretation is that the Curie term may result from Cu^{2+} ion substituting for the Tl site. If we assume that only the Cu^{2+} ion with spin $\frac{1}{2}$ and $g=2.2$ contributes the observed Curie term, the Cu^{2+} -to-Cu ratio is estimated to be $\sim 6\%$,¹⁶ which is too large to be ascribed only to impurity phases but quite agrees with the substitution ratio described above. In that case, because of a small radius of the Cu^{2+} ion, oxygen atoms surrounding it must be rearranged locally so as to make its coordination environment favorable. However, possible coexistence of Cu^+ ions cannot be ruled out because the Curie term decreases with decreasing excess oxygen, which suggests that the coordination environment of Cu^{2+} changes toward that of Cu^+ . For the highest- T_c sample with no excess oxygen, the hole carriers created by substitution of Cu in the formula of $(\text{Tl}_{0.95}\text{Cu}_{0.05})_2\text{Ba}_2\text{CuO}_{6+\delta}$ ($\delta \sim 0$) is 0.1–0.2 per Cu atom, which agrees with the typical value for other Cu-containing superconductors.

The present results do not necessarily exclude other possible origins of hole doping such as charge transfer between TlO and CuO_2 layers, which leads to the mixed-valency state of Tl^{3+} and Tl^+ . Such coexistence of Tl^{3+} and Tl^+ ions was proposed in an x-ray photoemission spectroscopy study of $\text{Tl}_2\text{Ba}_2\text{Ca}_2\text{Cu}_3\text{O}_{10}$ (Ref. 17), while only a Tl^{3+} signal was detected by ^{205}Tl NMR measurements.^{18,19} Though it still remains open whether such mixed valency occurs in this compound, the present study clearly reveals that a significant portion of the hole carriers in Tl 2:2:0:1 is attributed to the substitution of Cu for Tl and the uptake of excess oxygen at the interstitial site between the double TlO layers.

CONCLUSIONS

The presence of excess oxygen atoms located at the interstitial site between the double Tl-O layers in the Tl 2:2:0:1 compound were confirmed by neutron powder diffraction. The change in oxygen content and the corresponding change in hole concentration are caused by incorporation and release of the interstitial oxygen atoms. The amount of the excess oxygen decreases from ~ 0.1 to ~ 0 per formula unit as the sample changes from a normal metal to a superconductor with the T_c of 85 K.

About 5% of the Tl site is substituted by Cu. A significant portion of the hole carriers in the Tl 2:2:0:1 compound is attributed to the substitution of Cu for Tl and incorporation of the excess oxygen.

ACKNOWLEDGMENTS

We thank T. Satoh for the x-ray microanalysis and M. Sugimoto for experimental assistance. We also thank N. Shohata for the support of this work.

- ¹Y. Shimakawa, Y. Kubo, T. Manako, T. Satoh, S. Iijima, T. Ichihashi, and H. Igarashi, *Physica C* **157**, 279 (1989).
- ²Y. Kubo, Y. Shimakawa, T. Manako, T. Satoh, S. Iijima, T. Ichihashi, and H. Igarashi, *Physica C* **162-164**, 991 (1989).
- ³J. B. Torrance, Y. Tokura, A. I. Nazzal, A. Bezinge, T. C. Huang, and S. S. P. Parkin, *Phys. Rev. Lett.* **61**, 1127 (1988).
- ⁴T. Manako, Y. Shimakawa, Y. Kubo, T. Satoh, and H. Igarashi, *Physica C* **158**, 143 (1989).
- ⁵H. Takagi, T. Ido, S. Ishibashi, M. Uota, S. Uchida, and Y. Tokura, *Phys. Rev. B* **40**, 2254 (1989).
- ⁶J. B. Torrance, A. Bezinge, A. I. Nazzal, T. C. Huang, S. S. P. Parkin, D. T. Keane, S. J. LaPlaca, P. M. Horn, and G. A. Held, *Phys. Rev. B* **40**, 8872 (1989).
- ⁷Y. Shimakawa, Y. Kubo, T. Manako, and H. Igarashi, *Phys. Rev. B* **40**, 11 400 (1989).
- ⁸N. Watanabe, H. Asano, H. Iwasa, S. Satoh, H. Murata, K. Karahashi, S. Tomiyoshi, F. Izumi, and K. Inoue, *Jpn. J. Appl. Phys.* **26**, 1164 (1987).
- ⁹F. Izumi, H. Asano, H. Murata, and N. Watanabe, *J. Appl. Crystallogr.* **20**, 411 (1987).
- ¹⁰F. Izumi, *J. Crystallogr. Soc. Jpn.* **27**, 23 (1985) (in Japanese).
- ¹¹C. C. Torardi, M. A. Subramanian, J. C. Calabrese, J. Gopalakrishnan, E. M. McCarron, K. J. Morrissey, T. R. Askew, R. B. Flippen, U. Chowdhry, and A. W. Sleight, *Phys. Rev. B* **38**, 225 (1988).
- ¹²J. D. Jorgensen, B. Dabrowski, Shiyou Pei, D. G. Hinks, L. Soderholm, B. Morosin, J. E. Schirber, E. L. Venturini, and D. S. Ginley, *Phys. Rev. B* **38**, 11 337 (1988).
- ¹³J. D. Jorgensen, B. Dabrowski, Shiyou Pei, D. R. Richards, and D. G. Hinks, *Phys. Rev. B* **40**, 2187 (1989).
- ¹⁴J. B. Parise, C. C. Torardi, M. A. Subramanian, J. Gopalakrishnan, and A. W. Sleight, *Physica C* **159**, 239 (1989).
- ¹⁵M. Onoda, S. Kondoh, K. Fukuda, and M. Sato, *Jpn. J. Appl. Phys.* **27**, L1234 (1988).
- ¹⁶Y. Kubo, Y. Shimakawa, T. Manako, and H. Igarashi, in *Proceedings of the Second International Symposium on Superconductivity, Tsukuba, Japan, 1989*, edited by T. Ishiguro and K. Kajimura (Springer-Verlag, Tokyo, 1990).
- ¹⁷T. Suzuki, M. Nagoshi, Y. Fukuda, Y. Syono, M. Kikuchi, N. Kobayashi, and M. Tachiki, *Phys. Rev. B* **40**, 5184 (1989).
- ¹⁸F. Hentsch, N. Winzek, M. Mehring, H. J. Mattausch, A. Simon, and R. Kremer, *Physica C* **165**, 485 (1990).
- ¹⁹D. M. deLeeuw, W. A. Groen, J. C. Jol, H. B. Brom, and H. W. Zandbergen, *Physica C* **166**, 349 (1990).

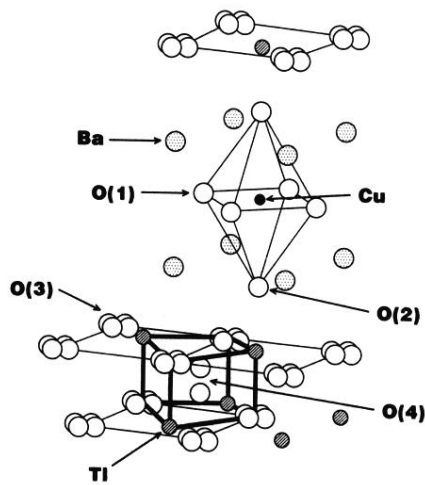


FIG. 2. Crystal structure of Tl 2:2:0:1. The O(3) atom is split into four pieces by assigning a $16n$ site deviating slightly from the ideal site. The O(4) atom is located at the interstitial site between double TlO layers. Each O(4) atom is coordinated to four Tl atoms, and is split into two pieces by assigning an $8g$ site.